

Supporting information

Trace element mobility impacted by Fe₃O₄-nanoparticles surface coating within wetland soil

Maya Al-Sid-Cheikh^{a,§*}, Mathieu Pédrot^a, Aline Dia^a, Mélanie Davranche^a, Laurent Jeanneau^a,
Patrice Petitjean^a, Martine Bouhnik-Le Coz^a, Marc-André Cormier^{b,c} and Fabien Grasset^{d,e}

Contents

Figure S 1. TEM images of uncoated and DMSA coated nano-Fe ₃ O ₄ (a) uncoated and (b) coated, respectively. C) Characterization of pH _{ZPC} of uncoated nFe ₃ O ₄ according to Bourikas, et al. (2003), called differential potentiometric titration (DPT) for uncoated nano-Fe ₃ O ₄ . Three replicates were performed called nano-Fe ₃ O _{4_a} , nano-Fe ₃ O _{4_b} and nano-Fe ₃ O _{4_c} .	2
Figure S 2. XRD images from a) uncoated nFe ₃ O ₄ and b) coated nFe ₃ O ₄ with d-spacing calculated for the four first circles (i.e. green dot) and the comparison with AMS database gives magnetite crystallography structure, with h k l: 4 0 0.	3
Figure S 3. Study site of the experimental watershed of Pleine-Fougères, Western France.	4
Figure S 4. Py-GCMS analyses for a) Control; b) nFe ₃ O ₄ uncoated and c) nFe ₃ O ₄ @DMSA. The labels are the percentage for each compound.	5
Figure S5. Mass leached < 200 nm of copper (Cu), Arsenic (As), Aluminum (Al), Uranium (U), Strontium (Sr) and Rare Earth Elements (REE) during each leaching.	6
Table S1. Magnetite AMS sheet from Haavik C, Stolen S, Fjellvag H, Hanfland M, Hausermann D, American Mineralogist 85 (2000) 514-523, Equation of state of magnetite and its high-pressure modification: Thermodynamics of the Fe-O system at high pressure (database: # amcsd 0002411). http://serc.carleton.edu/	7
Table S 2. Trace elements analysis on nano-Fe ₃ O ₄ uncoated and coated	8
Table S3. Key properties of soil grain size mixtures A	9
Table S 4. Element analysis of the soil fraction A.	10
Table S5. Initial composition of the leaching solution for three exposures and the triplicates. L.D is limit of detection.	11
Table S6. Total amount of Organic carbon and Iron < 220nm during the soil leaching experiments.	12
Analysis 1 SUVA and Aromaticity treatment	13
Analysis 2 Procedure and data treatment for Py-GCMS analysis	14

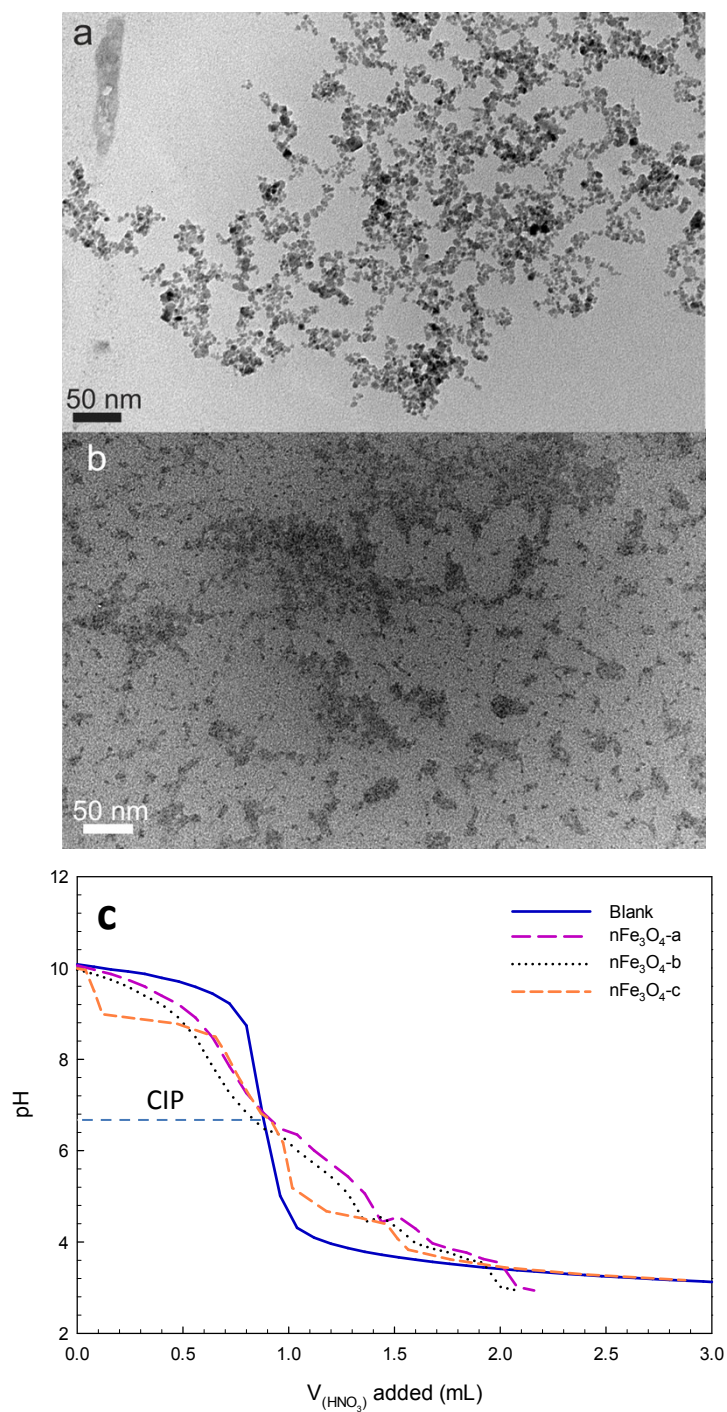


Figure S 1. TEM images of uncoated and DMSA coated nano-Fe₃O₄ (a) uncoated and (b) coated, respectively. C) Characterization of pH_{ZPC} of uncoated nano-Fe₃O₄ according to Bourikas, et al. (2003), called differential potentiometric titration (DPT) for uncoated nano-Fe₃O₄. Three replicates were performed called nano-Fe₃O₄_a, nano-Fe₃O₄_b and nano-Fe₃O₄_c. Abbreviation: CIP, Common intersection point.

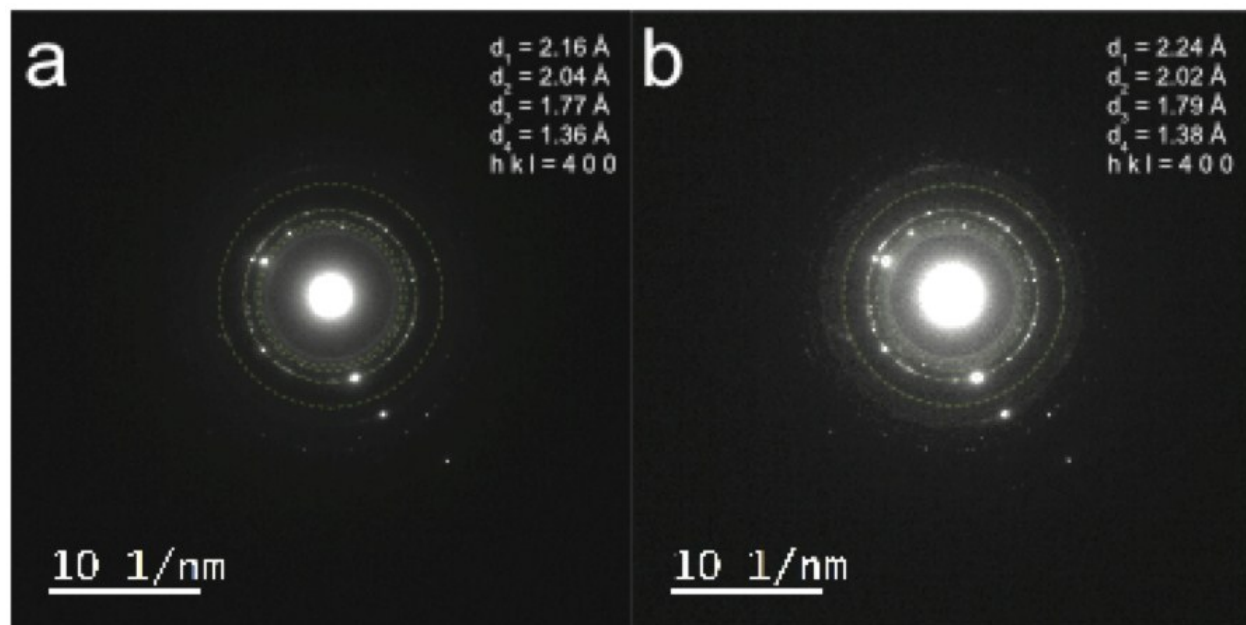


Figure S 2. XRD images from a) uncoated $n\text{Fe}_3\text{O}_4$ and b) coated $n\text{Fe}_3\text{O}_4$ with d-spacing calculated for the four first circles (i.e. green dot) and the comparison with AMS database gives magnetite crystallography structure, with hkl: 4 0 0.

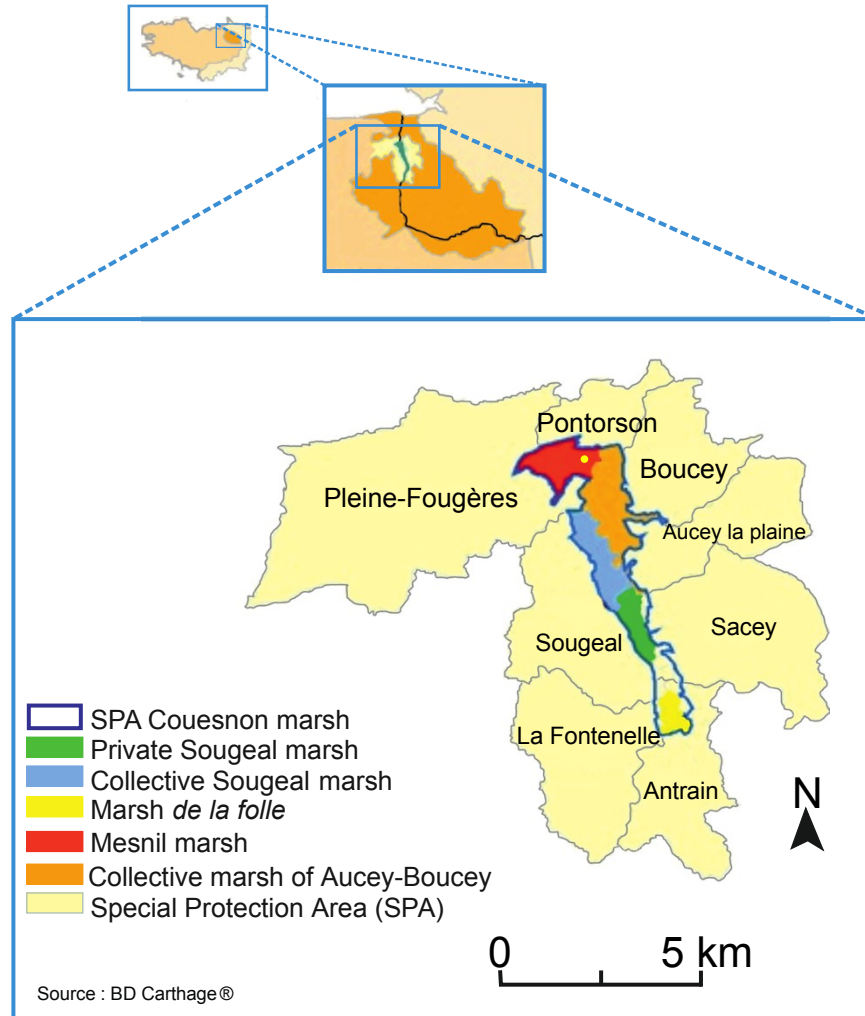


Figure S 3. Study site of the experimental watershed of Pleine-Fougères, Western France. The soil was collected at the location 48°31'20.5"N 1°33'38.4"W (yellow dot), next to the '*Ruisseau du petit Hermitage*'.

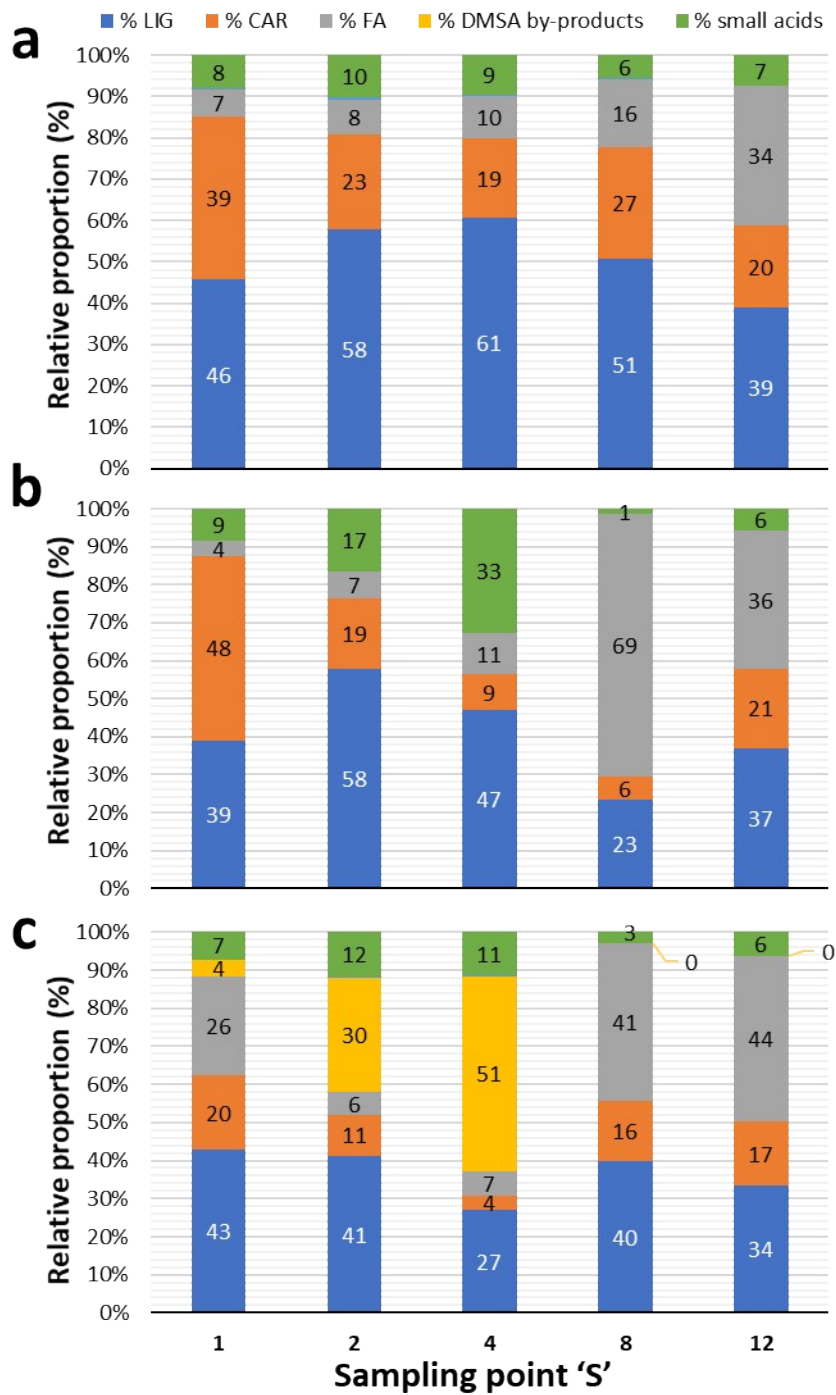


Figure S 4. Py-GCMS analyses for a) Control; b) nFe₃O₄ uncoated and c) nFe₃O₄@DMSA. The labels are the percentage for each compound.

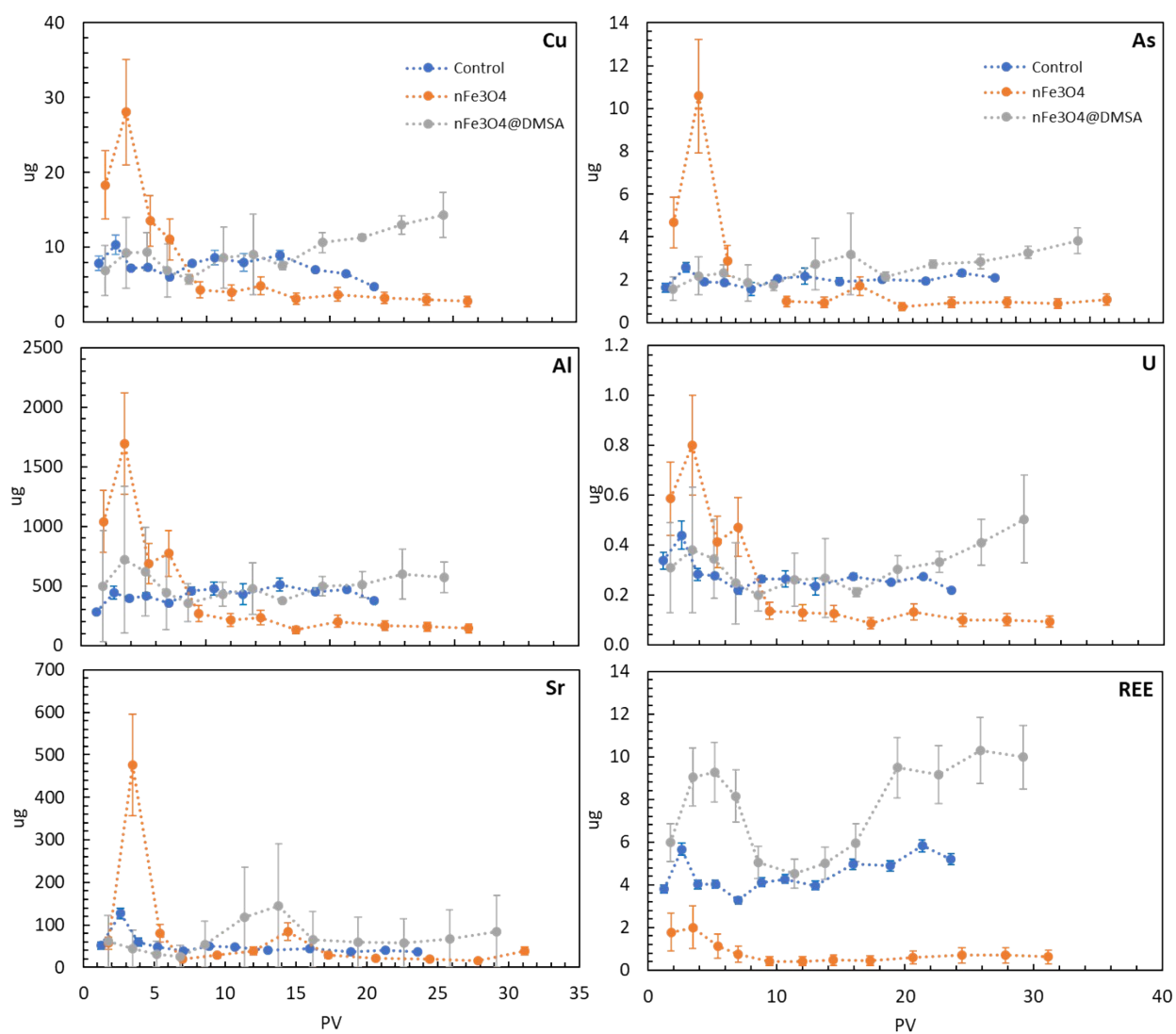


Figure S5. Mass leached < 200 nm of copper (Cu), Arsenic (As), Aluminum (Al), Uranium (U), Strontium (Sr) and Rare Earth Elements (REE) during each leaching.

Table S1. Magnetite AMS sheet from Haavik C, Stolen S, Fjellvag H, Hanfland M, Hausermann D, American Mineralogist 85 (2000) 514-523, Equation of state of magnetite and its high-pressure modification: Thermodynamics of the Fe-O system at high pressure (database: # amcsd 0002411). <http://serc.carleton.edu/>

2-THETA	INTENSITY	D-SPACING	H	K	L	Multiplicity
18.77	8.68	4.728	1	1	1	8
30.88	28.49	2.8953	2	2	0	12
36.39	100	2.4691	3	1	1	24
38.07	8.6	2.364	2	2	2	8
44.24	19.65	2.0473	4	0	0	6
54.93	9.09	1.6716	4	2	2	24
58.57	5.95	1.576	3	3	3	8
58.57	24.11	1.576	5	1	1	24
64.35	38.84	1.4476	4	4	0	12
73.08	3.19	1.2948	6	2	0	24
76.24	8.1	1.2488	5	3	3	24
77.28	3.87	1.2346	6	2	2	24
81.42	2.41	1.182	4	4	4	8
89.57	3.51	1.0943	6	4	2	48
18.77	8.68	4.728	1	1	1	8
30.88	28.49	2.8953	2	2	0	12

Cell parameters: 8.1891; 8.1891; 8.1891; 90.000; 90.000; 90.000; Space group: Fd3m; X-ray wavelength: 1.541838; MAX. ABS. Intensity / Volume**2: 97.1243910

Table S 2. Trace elements analysis on nano-F₃O₄ uncoated and coated

	Uncoated	Coated		Uncoated	Coated
	$\mu\text{g L}^{-1}$			$\mu\text{g L}^{-1}$	
Li	0.01	0.00	La	0.007	0.01
Be	0.00	0.00	Ce	0.0007	0.00
B	0.46	0.00	Pr	3.8×10^{-5}	0.00
Mg	0.73	3.92	Nd	0.0005	0.00
Al	1.22	10.66	Sm	9.3×10^{-5}	0.00
K	12.00	0.00	Eu	0.0003	0.00
Ca	3.75	18.07	Gd	<LD	0.00
Sc	0.01	0.00	Tb	9.4×10^{-5}	0.00
V	0.00	0.02	Dy	<LD	0.00
Cr	0.37	1.35	Ho	<LD	0.00
Mn	4.09	15.39	Er	<LD	0.00
Co	0.12	0.45	Tm	2.9×10^{-6}	0.00
Ni	2.84	5.50	Yb	1.7×10^{-5}	0.00
Cu	0.88	2.64	Lu	<LD	0.00
Zn	0.31	2.45	Pb	0.07	0.07
Ga	0.00	0.02	Th	0.007	0.01
As	0.00	0.10	U	6.2×10^{-5}	0.00
Rb	0.01	0.00			
Sr	0.04	0.31			
Y	0.00	0.01			
Cd	0.00	0.01			
Sb	0.01	0.03			
Ba	0.06	0.26			

Table S3. Key properties of soil grain size mixtures A

Soil fraction	Air dry moisture (%)	SOM (%)	CEC (meq/100 g)	pH_{soil}	Nitrogen (g/kg)	C/N	S_{Total} (%)	Sand (%)	Silt (%)	Clay (%)
A	3.2	8.5	20.4	5.0	4.5	11	0.07	9.9	69.2	20.9

Table S 4. Element analysis of the soil fraction A.

<i>Element</i>	<i>ppm</i>	<i>Element</i>	<i>ppm</i>	<i>Element</i>	<i>%</i>
As	7.3	Nb	10.5	SiO₂	61.5
Ba	406.3	Nd	24.7	Al₂O₃	11.6
Be	1.7	Ni	32.0	Fe₂O₃	3.6
Bi	0.2	Pb	23.2	MnO	0.04
Cd	0.3	Pr	6.1	MgO	0.9
Ce	55.4	Rb	66.8	CaO	0.5
Co	9.5	Sc	11.8	Na₂O	0.9
Cr	82.8	Sb	0.9	K₂O	1.8
Cs	4.3	Sm	5.0	TiO₂	0.7
Cu	21.0	Sn	3.0	P₂O₅	0.2
Dy	4.3	Sr	59.3	PF	18.0
Er	2.5	Ta	0.9	Total	99.6
Eu	1.0	Tb	0.7		
Ga	14.8	Th	7.8		
Gd	4.4	Tm	0.4		
Ge	1.4	U	2.7		
Hf	6.8	V	77.5		
Ho	0.9	W	1.6		
In	< L.D.	Y	24.1		
La	26.1	Yb	2.6		
Lu	0.4	Zn	76.3		
Mo	0.7	Zr	269.9		

Table S5. Initial composition of the leaching solution for three exposures and the triplicates. L.D is limit of detection.

# ID	<i>Leaching solution</i>				<i>Column parameters</i>						
	C _{org} (mg L ⁻¹)	Fe (mg L ⁻¹)	pH	T °C	d (g cm ⁻¹)	Flow rate (mL min ⁻¹)	PV mL	m _{soil} g	H cm	Fe ₂ O ₃ g	Fe
Blank a	0.06	<L.D.	6.5	20	0.58	5.21 ± 0.3	300	275	37.5	9.9	3.5
Blank b	0.03	<L.D.	6.5	20	0.61	5.25 ± 0.4	294	292.6	38	10.5	3.7
Blank c	0.02	<L.D.	6.5	20	0.59	5.09 ± 0.2	284	276.9	37.5	10.0	3.5
nFe₃O₄ a	0.21	39.8±1.2	6.5	20	0.6	5.17 ± 0.5	295	285.9	38	10.3	3.6
nFe₃O₄ b	0.18	41.1±0.9	6.5	20	0.59	5.42 ± 0.3	294	281.3	38	10.1	3.5
nFe₃O₄ c	0.23	38.6±0.7	6.5	20	0.61	5.07 ± 0.3	324	290.4	38	10.5	3.7
nFe₃O₄@DMSA a	305.7	41.3±0.8	6.5	20	0.57	5.4 ± 0.2	308	270	38	9.7	3.4
nFe₃O₄@DMSA b	287.9	38.9±1.1	6.5	20	0.56	5.8 ± 0.5	300	268	38	9.6	3.4
nFe₃O₄@DMSA c	300.5	40.6±1.0	6.5	20	0.54	5.2 ± 0.3	320	258	38	9.3	3.2

Table S6. Total amount of dissolved organic carbon and iron < 220nm during the soil leaching experiments.

	<i>Avg</i>	<i>PV</i>	<i>s.d.</i>	<i>DOC</i> (<i>mg</i>)	<i>s.d.</i>	<i>Fe</i> (μ <i>g</i>)	<i>s.d.</i>
<i>Control-S1</i>	1.2	0.078	131.3	11.5	468.0	46.2	
<i>Control-S2</i>	2.6	0.202	174.6	28.4	566.5	65.4	
<i>Control-S3</i>	3.9	0.222	92.5	11.6	499.5	1.8	
<i>Control-S4</i>	5.2	0.189	81.2	14.6	561.6	34.7	
<i>Control-S5</i>	7.0	0.280	62.1	4.7	440.0	14.0	
<i>Control-S6</i>	8.8	0.437	74.2	6.2	554.3	38.2	
<i>Control-S7</i>	10.7	0.549	69.1	8.7	493.9	64.3	
<i>Control-S8</i>	13.0	0.611	54.4	6.7	315.9	32.2	
<i>Control-S9</i>	15.9	0.688	65.6	4.2	291.8	16.5	
<i>Control-S10</i>	18.8	0.764	61.2	7.8	295.0	26.2	
<i>Control-S11</i>	21.3	0.869	68.7	5.5	412.5	34.8	
<i>Control-S12</i>	23.5	0.962	57.5	2.9	456.3	32.4	
Total			992.5	113.1	5355.3	406.7	
<i>nFe₃O₄-S1</i>	1.8	0.09	138.72	56.07	694.42	166.88	
<i>nFe₃O₄-S2</i>	3.5	0.07	97.22	13.82	1182.35	372.96	
<i>nFe₃O₄-S3</i>	5.4	0.37	62.47	20.35	668.31	271.27	
<i>nFe₃O₄-S4</i>	7.0	0.22	34.52	2.25	357.37	41.26	
<i>nFe₃O₄-S5</i>	9.4	0.24	30.48	4.55	174.15	50.78	
<i>nFe₃O₄-S6</i>	12.0	0.21	22.45	1.43	110.14	2.09	
<i>nFe₃O₄-S7</i>	14.4	0.49	18.83	0.49	112.09	16.99	
<i>nFe₃O₄-S8</i>	17.3	0.41	20.71	4.11	89.19	50.32	
<i>nFe₃O₄-S9</i>	20.6	0.50	24.37	0.87	79.02	27.78	
<i>nFe₃O₄-S10</i>	24.4	0.83	30.42	5.06	93.44	37.32	
<i>nFe₃O₄-S11</i>	27.8	0.83	29.22	2.57	120.30	9.35	
<i>nFe₃O₄-S12</i>	31.1	0.72	27.07	1.68	161.87	23.22	
Total			536.5	113.2	3842.6	1070.2	
<i>nFe₃O₄@DMSA-S1</i>	1.7	0.05	160.3	21.2	1228.7	151.2	
<i>nFe₃O₄@DMSA-S2</i>	3.5	0.10	242.4	54.5	2836.1	526.5	
<i>nFe₃O₄@DMSA-S3</i>	5.1	0.07	259.7	78.5	4177.7	512.8	
<i>nFe₃O₄@DMSA-S4</i>	6.8	0.14	257.8	81.9	3541.2	605.3	
<i>nFe₃O₄@DMSA-S5</i>	8.6	0.20	193.7	62.4	1681.1	180.3	
<i>nFe₃O₄@DMSA-S6</i>	11.4	0.46	104.4	29.3	884.2	173.2	
<i>nFe₃O₄@DMSA-S7</i>	13.8	0.49	46.9	12.5	874.4	241.9	
<i>nFe₃O₄@DMSA-S8</i>	16.2	0.55	56.9	13.4	998.1	334.9	
<i>nFe₃O₄@DMSA-S9</i>	19.4	0.75	84.9	15.1	1088.6	388.3	
<i>nFe₃O₄@DMSA-S10</i>	22.6	0.95	105.6	19.2	1130.6	419.4	
<i>nFe₃O₄@DMSA-S11</i>	25.8	1.09	104.4	25.6	1316.1	505.9	
<i>nFe₃O₄@DMSA-S12</i>	29.2	1.3	131.0	36.0	1274.5	487.8	
Total			1748.0	449.5	21031.3	4527.6	

Analysis 1 SUVA and Aromaticity treatment

A normalized parameter of specific ultraviolet absorbance (SUVA), which is calculated as the ratio between the UVA at a given wavelength and the organic carbon content, has been applied in water chemistry (Traina et al., 1990; Weishaar et al., 2003).

Thus, absorbance at 254 nm was measured to obtain SUVA (specific ultra-violet absorbance, eq. 1) values in according to:

$$SUVA = \frac{A_{254nm}}{[OC]}$$

The values of SUVA determined at 254 nm can be used to describe the composition of water in terms of hydrophobicity and hydrophilicity, and $SUVA_{254} > 4 \text{ L mg}^{-1} \text{ m}^{-1}$ indicates mainly hydrophobic and especially aromatic material, whereas $SUVA_{254} < 3 \text{ L mg}^{-1} \text{ m}^{-1}$ represents hydrophilic material (Edzwald et al., 1985).

The values of $SUVA_{254}$ were found to be strongly correlated with percent aromaticity for organic matter isolated from aquatic environment (Weishaar et al., 2003) in according to:

$$Aromaticity = 6.52 \times SUVA + 3.63$$

These parameters were used such as an indicator of the chemical composition of the leached NOM.

Analysis 2 Procedure and data treatment for Py-GCMS analysis

Approximately 2 mg of solid residue (lyophilizate) were introduced into an 80 μ L aluminum reactor with an excess of solid tetramethylammonium hydroxide (TMAH – ca. 10 mg). The THM reaction was performed on-line using a vertical micro-furnace pyrolyser PZ-2020D (Frontier Laboratories, Japan) operating at 400°C during 1 min. The products of this reaction were injected into a gas chromatograph (GC) GC-2010 (Shimadzu, Japan) equipped with a SLB 5MS capillary column (60 m \times 0.25 mm ID, 0.25 μ m film thickness) in the split mode. The split ratio was adapted according to the sample and ranged from 10 to 30. The temperature of the transfer line was 321°C and the temperature of the injection port was 310°C. The oven temperature was programmed from an initial temperature of 50°C (held for 2 min) rising to 150°C at 7°C/min, then rising from 150°C to 310°C (held for 20 min) at 4°C/min. Helium was used as the carrier gas, with a flow rate of 1.0 ml/min. Compounds were detected using a QP2010+ mass spectrometer (MS) (Shimadzu, Japan) operating in the full scan mode. The temperature of the transfer line was set at 280°C, and molecules were ionized by electron impact using energy of 70 eV. The temperature of the ionization source was set at 200°C. The list of analyzed compounds and m/z ratios used for their integration are given in the supplementary materials (Table S1). Compounds were identified on the basis of their full-scan mass spectra by comparison with the NIST library and with published data. They were classified into three categories: lignin (LIG) and tannin (TAN) markers, carbohydrates (CAR) and fatty acids (FA). The peak area of the selected m/z for each compound was integrated and corrected by a mass spectra factor (MSF) calculated as the reciprocal of the proportion of the fragment (used for the integration) relating to the entire fragmentogram provided by the NIST library.

LIG were quantified using an internal calibration for 3,4-dimethoxybenzoic acid methyl ester, 3-(4-methoxyphenyl)-prop-2-enoic acid, methyl ester and 3,4,5-trimethoxybenzoic acid methyl ester. Dihydrocinnamic acid d9 methyl ester (CDN Isotopes, D5666) was used as an internal standard and was added to the system prior to the THM step (10 μ L of a 25 ppm solution in methanol). The other LIG and TAN compounds were quantified by assuming that their quantification factors were similar to those of 3,4-dimethoxybenzoic acid methyl ester. For this type of analysis, the relative standard deviation (RSD) represents approximately 10% of the values.

The proportion of each compound class was calculated by dividing the sum of the areas of the compounds in this class by the sum of the peak areas of all analyzed compounds multiplied by 100 in order to express it as a percentage. The use of THM-GC-MS to investigate the temporal variability of the DOM composition meant that it was necessary to assume that the ionization efficiency and matrix effects are equivalent for all analyzed compounds in all samples.

Treatment of molecular data

The classification of molecular markers generated by THM-GC-MS into microbial and plant-derived markers has been performed according to Jeanneau et al. (2014). Briefly, the analyzed compounds were classified as follows. LIG-TAN are characteristic of DOM inherited from plant-derived inputs, whereas CAR and FA can be inherited from both plant-derived and microbial sources. The proportion of microbial CAR was calculated using an end-member mixing approach (EMMA) based on the deoxyC6/C5 ratio, assuming that it is 0.5 and 2.0 for plant-derived and microbial inputs, respectively (Rumpel and Dignac, 2006). C6 were not considered since they can derive from the THM of cellulose leading to an increase of the plant-derived C6 signal. The proportion of microbial FA was calculated as the % low molecular weight FA (< C19) by excluding C16:0 and C18:0 that can be inherited from plant-derived or microbial inputs. The microbial FA were composed of C12:0, C13:0, C14:0, C15:0, C17:0, anteiso and iso C15:0 and C17:0, iso C16:0, C16:1 and C18:1 commonly used as bacterial indicators (Frostegård et al., 1993). The proportion of microbial markers was calculated as the sum of the proportion of microbial CAR multiplied by the proportion of CAR plus the proportion of microbial FA multiplied by the proportion of FA. From this value, it is possible to calculate the proportion of plant-derived markers among the analyzed compounds. For this calculation, it is assumed that the modification of the distribution of CAR and FA would only be due to the relative proportion between these plant-derived and microbial inputs. Although these assumptions still need to be validated by investigating pure and known mixtures of vegetal and microbial sources, this approach can be used to approximate the proportions of plant-derived and microbial CAR.

- K. Bourikas, J. Vakros, C. Kordulis and A. Lycourghiotis, 2003. Potentiometric Mass Titrations: Experimental and Theoretical Establishment of a New Technique for Determining the Point of Zero Charge (PZC) of Metal (Hydr)Oxides. *Journal of Physical Chemistry B*, 107, 9441–9451.
- Edzwald, J.K., Becker, W.C., Wattier, K.L., 1985. Surrogate Parameters for Monitoring Organic Matter and THM Precursors. *Journal (American Water Works Association)* 77, 122-132.
- Frostegård, Å., Tunlid, A., Bååth, E., 1993. Phospholipid Fatty Acid Composition, Biomass, and Activity of Microbial Communities from Two Soil Types Experimentally Exposed to Different Heavy Metals. *Applied and Environmental Microbiology* 59, 3605-3617.
- Jeanneau, L., Jaffrezic, A., Pierson-Wickmann, A.-C., Gruau, G., Lambert, T., Petitjean, P., 2014. Constraints on the Sources and Production Mechanisms of Dissolved Organic Matter in Soils from Molecular Biomarkers. *Vadose Zone Journal* 13.
- Rumpel, C., Dignac, M.-F., 2006. Gas chromatographic analysis of monosaccharides in a forest soil profile: Analysis by gas chromatography after trifluoroacetic acid hydrolysis and reduction–acetylation. *Soil Biology and Biochemistry* 38, 1478-1481.
- Stevenson, F.J., 1982. *Humus Chemistry. Genesis, Composition, Reactions.*, New York.
- Tam, S.C., Sposito, G., 1993. Fluorescence spectroscopy of aqueous pine litter extracts: effects of humification and aluminium complexation. *Journal of Soil Science* 44, 513-524.
- Traina, S.J., Novak, J., Smeck, N.E., 1990. An Ultraviolet Absorbance Method of Estimating the Percent Aromatic Carbon Content of Humic Acids. *Journal of Environmental Quality* 19, 151-153.
- Weishaar, J.L., Aiken, G.R., Bergamaschi, B.A., Fram, M.S., Fujii, R., Mopper, K., 2003. Evaluation of Specific Ultraviolet Absorbance as an Indicator of the Chemical Composition and Reactivity of Dissolved Organic Carbon. *Environmental Science & Technology* 37, 4702-4708.
- Zsolnay, A., Baigar, E., Jimenez, M., Steinweg, B., Saccomandi, F., 1999. Differentiating with fluorescence spectroscopy the sources of dissolved organic matter in soils subjected to drying. *Chemosphere* 38, 45-50.